Extended Eden model reproduces growth of an acellular slime mold

Geri Wagner,[1,*] Ragnhild Halvorsrud,[2] and Paul Meakin[1]
[1]*Department of Physics, University of Oslo, Box 1048 Blindern, N-0316 Oslo, Norway*
[2]*Institute of Physiology, University of Oslo, Box 1103 Blindern, N-0316 Oslo, Norway*
(Received 22 February 1999)

A stochastic growth model was used to simulate the growth of the acellular slime mold *Physarum polycephalum* on substrates where the nutrients were confined in separate drops. Growth of *Physarum* on such substrates was previously studied experimentally and found to produce a range of different growth patterns [Phys. Rev. E **57**, 941 (1998)]. The model represented the aging of cluster sites and differed from the original Eden model in that the occupation probability of perimeter sites depended on the time of occupation of adjacent cluster sites. This feature led to a bias in the selection of growth directions. A moderate degree of persistence was found to be crucial to reproduce the biological growth patterns under various conditions. Persistence in growth combined quick propagation in heterogeneous environments with a high probability of locating sources of nutrients. [S1063-651X(99)16210-X]

PACS number(s): 87.18.Bb

I. INTRODUCTION

Simple algorithmic models have proved to be extremely useful to illustrate fundamental aspects of growth and development of biological systems. The main challenge in devising such a model is to identify the critical factors that determine the complex patterns exhibited by even the most simple biological systems. For instance, Eden [1] presented a model for the spreading of bacterial colonies on a homogeneous substrate. The Eden model is a stochastic growth model in which the substrate is represented by a lattice of sites, and the colony is represented by a cluster of labeled sites (occupied sites). In each growth step, one of the unoccupied sites at the perimeter of the cluster is chosen at random and occupied. The resulting cluster is compact and has a self-affine front, or active zone [2,3].

Since the pioneering work of Eden, a wide variety of related models have been developed in order to simulate more realistically both biological and nonbiological growth processes. The first of these was a model for skin cancer introduced by Williams and Bjerknes [4]. In this model, unoccupied perimeter sites can be occupied and occupied perimeter sites can be emptied, with different probabilities to represent the biased competition between the growth of cancerous cells and the growth of normal cells. Recently, more sophisticated models have been developed for the growth of bacterial colonies [5–9], fungal mycelia [10,11], and a variety of other cellular activities and biological pattern formation processes [12–21].

Modeling studies of pattern formation, cell communication, and aggregation have been reported for the cellular slime mold *Dictyostelium discoideum* [22–24]. In the present paper, we focus on the plasmodial growth in the *acellular* slime mold *Physarum polycephalum*. To our knowledge, no computer models for growth and pattern formation in *Physarum* have been described in the scientific literature. *Physarum* has some features that make it very attractive for laboratory experimental studies: The stages of proliferation and differentiation are easily distinguishable [25], and it can be cultured throughout its entire life cycle.

In its plasmodial stage, the multinucleated *Physarum* forms a single giant cell that can measure several inches or more in diameter [26]. Given an ample supply of nutrients, the plasmodium is completely sedentary and has the appearance shown in Fig. 1(a). Under these conditions it grows steadily and approximately isotropically, interrupted every 10–14 hours by synchronous nuclear division [27,28]. The plasmodium is composed of interconnected veins embedded in a continuous plasmodial sheet, each vein consisting of an ectoplasmic tube surrounding a core of fluid endoplasm. Regular contractions generated by contractile activities in the ectoplasm results in a reversible endoplasmic streaming [29]. In environments providing poor nutrition, the plasmodium is capable of migration and organizes into a fan-shaped front with a propagation velocity of up to a few centimeters per hour [30,31]. Figure 1(b) shows a migrating *Physarum*.

Recently, we studied the growth of *Physarum* experimentally using substrates on which the nutrients were confined in separated agar medium drops with diameters between 0.5 and about 1 cm [32,33]. Although the drops in the substrate had a height of 2–3 mm we have ignored any gravitational effects and considered the system as being purely two-dimensional. On these nonuniform substrates the plasmodium develops near the borderline between the sedentary and the migratory regime. A ''searching phase'' in which the plasmodium explored the empty space between nutrient-containing drops, and a ''feeding phase'' in which nutrients from a fresh drop were absorbed, could be distinguished. Isotropic expansion in the nutrient-free regions ceased when the searching structure made contact with a fresh drop, and the drop was covered quickly with dense plasmodial structure. After a drop had been covered, the plasmodium again formed searching structures that expanded almost isotropically from the covered drops, which continued to supply nutrients.

*Present address: School of Astronomy and Physics, Raymond and Beverly Sackler Faculty of Exact Sciences, Tel Aviv University, Ramat Aviv 69978, Tel Aviv, Israel.

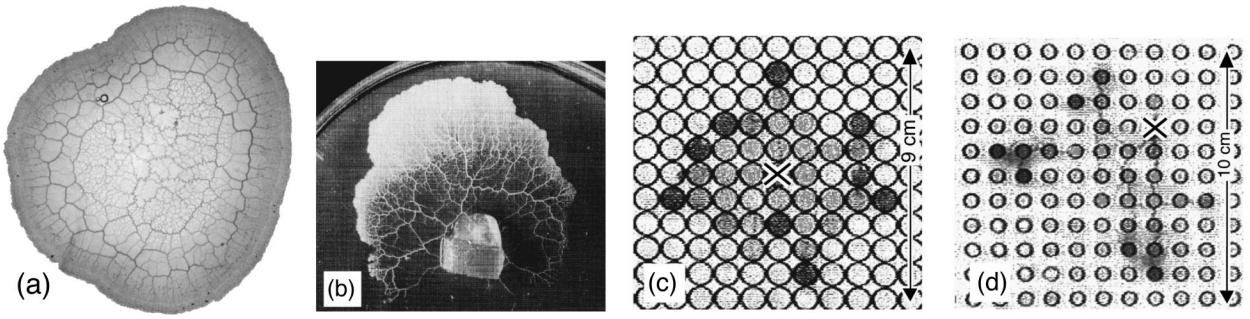

FIG. 1. (a) *Physarum* growing on a uniform substrate of agar measuring approximately 12 cm in diameter. (b) A starved plasmodium (diameter approximately 5 cm) develops a polarized structure and migrates over the substrate by amoeboid motion. (c) and (d) *Physarum* (dark structure) growing on a substrate of separate drops of agar medium, at early stages of the experiments. The most recently invaded parts are shown darkest. Inactive parts of the plasmodium are transparent. The inoculation drops are marked by a cross.

A transition in the *Physarum* growth morphology could be observed on nonuniform substrates [33]. The drops covered by the slime mold formed a compact roundish cluster when about 2/3 of the substrate area were covered by nutrients. However, the plasmodium did not attain the nearly regular, circular shape characterizing a sedentary slime mold growing on a uniform substrate of agar. If the nutrient drop coverage was reduced to about 1/4, the plasmodium expanded quite asymmetrically, and a branched, ramified cluster of invaded drops was formed. The drop size is a crucial parameter that modifies the characteristic plasmodial morphologies. Figure 1(c) shows a plasmodium growing on a drop substrate with large drops, providing a high coverage of nutrients, and Fig. 1(d) shows a plasmodium growing on a substrate with small drops. The key observations reported in Ref. [33] are

(i) The plasmodium expands steadily and almost isotropically on a uniform substrate with sufficient nutrients.

(ii) On a drop substrate, the plasmodium alternates between ''feeding phases'' in which a fresh drop is covered rapidly, and ''searching phases'' in which fresh drops are located by plasmodial expansion in nutrient-free regions.

(iii) If the nutrient-containing drops are arranged to form a line of equally separated drops, one drop after another is invaded, and the plasmodium grows along the line if the separation between the drops is not too large. Fresh drops are invaded at fairly regular intervals after a transient stage.

(iv) If the nutrient-containing drops are arranged to form a square lattice, branched or compact growth morphologies develop, depending on the drop size. If drops of intermediate sizes are used, cross-overs from branched to compact growth may occur.

Many essential biochemical aspects of growth of *Physarum* have been well elucidated in early literature (see Ref. [34] for a review). However, the interplay between microscopic processes at the subcellular level and growth and development of the plasmodium on a macroscopic scale needs to be clarified. The observations mentioned above may be helpful in this respect, since they are amenable to comparison with numerical growth models. Comparisons of real plasmodia and simulated plasmodia can be carried out in the context of growth patterns, defined by the number of covered drops and their spatial distribution, rather than in terms of absolute time and length. This implies that it is not necessary to calibrate the numerical model in terms of physical units. In this paper, we are concerned with a model for the growth of *Physarum* that was designed with comparisons of this sort in mind. In Sec. II we present a modified Eden growth model that was developed for this purpose, and compare the model with experimental observations of individual plasmodia in Sec. III. In Sec. IV we explore some selected properties of the model, and in Sec. V we discuss our results.

II. SIMULATION MODEL

A square lattice of sites was used to represent the entire substrate (both nutrient-containing and nutrient-free regions). Each site initially carried an amount n_0 of nutrients when the model was used to simulate growth on a uniform substrate of nutrients. In the simulations of growth on a drop substrate, a drop was represented by a cluster of 75 or more nutrient-carrying sites with a perimeter that approximated a circle, whereas the space between the drops was represented by nutrient-free sites.

Figures 2(a)–2(c) illustrate the growth model on a uniform substrate, and Figs. 2(d)–2(f) illustrate the growth on a non-uniform substrate. To begin a simulation, all but one sites were considered to be unoccupied. One of the nutrient-carrying sites was chosen as the seed site (the first site to be filled) of a cluster. Plasmodial growth was represented by successive growth steps. In each step an unoccupied lattice site adjacent to an occupied site was selected randomly and occupied to form a growing cluster. The probability P_j that a given unoccupied perimeter site j was selected and occupied depended on the ''age'' ϵ of the cluster sites i_j that were nearest neighbors to j. To find P_j, the sum

$$p_j = \sum_{i_j} \epsilon_{i_j}^{-\alpha} \quad (\epsilon_{i_j} < \epsilon_{max}), \tag{1}$$

was evaluated, where $\alpha \geqslant 0$ was a model parameter. The sum run over all cluster sites i_j that were nearest neighbors of the unoccupied perimeter site j, and whose age ϵ_{i_j} was lower than an upper limit ϵ_{max}. The normalized occupation probability $0 \leqslant P_j \leqslant 1$ was then given by

$$P_j = p_j \Big/ \sum_{k=1}^{N_a} p_k, \tag{2}$$

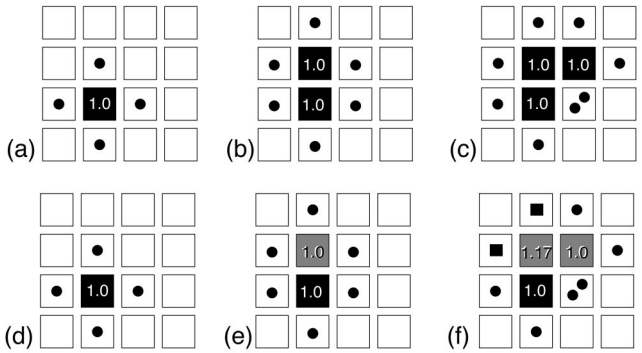

FIG. 2. Illustration of simulated plasmodial growth during the first three steps, on a uniform substrate [(a)–(c)], and on a nonuniform substrate on which nutrients are present and can be absorbed only at the seed site [(d)–(f)]. The age ϵ of the occupied sites is indicated. In (a) and (d), the plasmodium is shown in the first step, with one occupied site of age $\epsilon=1.0$. Each of the four unoccupied perimeter sites (dots) can be invaded with equal probability $p=1/4$ in the next step. (b) and (e) show the plasmodium in the second step. Each of the six unoccupied perimeter sites can be invaded with an equal probability of $p=1/6$. (c) shows the plasmodium in the third step on the uniform substrate. Six of the seven unoccupied perimeter sites can be occupied, each with the probability $p=1/8$. The seventh site (two dots) is adjacent to two covered sites and can be invaded in two ways. The total occupation probability for that site is $p=1/4$. On the non-uniform substrate [(f)], sites on which nutrient absorption is not possible (shaded) begin to age. The invasion probabilities for perimeter sites with single dots and squares are $p=1/P$ and $1.17^{-\alpha}/P$, respectively, with $P=6+2\cdot 1.17^{-\alpha}$. The site marked with two dots can be invaded in two ways, and the total probability is $p=2/P$.

where the index k labels all the N_a unoccupied perimeter sites. ($p_k=0$ for unoccupied perimeter sites that are nearest neighbors of only occupied sites with ages equal to ϵ_{max}). This model is closely related to the Eden model [1–3], and for $\alpha=0$, it is equivalent to ''Eden model C'' [3,35] in which unoccupied perimeter sites are randomly selected and occupied with probabilities proportional to the number of their occupied nearest neighbors.

A time scale was incorporated into the model to represent aging of the plasmodium. A time interval

$$\Delta t = 1/s \tag{3}$$

elapsed during each step in a simulation, where s denotes the number of possible growth steps at each stage. On a uniform substrate covered with nutrients, this time scale implies that the cluster size S (the number of occupied sites) increases quadratically in time in the early stages of growth. In the asymptotic limit, $S(t)\sim t^2$. In experiments, the area of a sedentary slime mold was found to increase approximately quadratically in time [36], consistent with the time scale used here. (In contrast, $\Delta t=$const would correspond to a constant growth rate and an increase of cluster size linear in time).

In each simulation step, an amount Δn of nutrients was ''absorbed'' at all the nutrient-carrying cluster sites. The amount of absorbed nutrients was proportional to the time

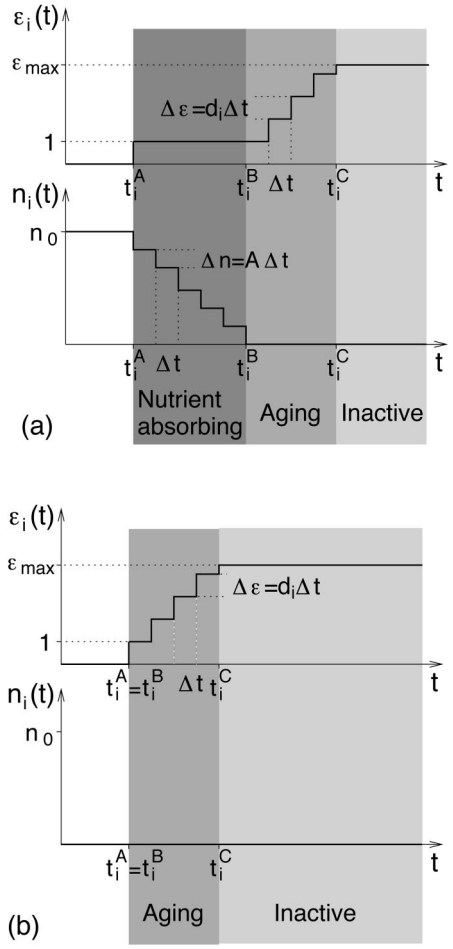

FIG. 3. Temporal development of the age $\epsilon_i(t)$ and the nutrient stock $n_i(t)$ for a nutrient-carrying cluster site (top) and a nutrient-free cluster site (bottom), respectively. After occupation at time t_i^A the age ϵ_i remains equal to unity while nutrients are absorbed at a constant rate. After depletion of the nutrients the age increases up to the maximum value ϵ_{max}, when the site becomes inactivated. Nutrient-free sites begin to age immediately after invasion.

interval, $\Delta n=A\Delta t$, representing a constant absorption rate. At each stage, the remaining amount of nutrients at the ith occupied site was given by

$$n_i(t)=\begin{cases} n_0, & t\leqslant t_i^A, \\ n_0-A(t-t_i^A), & t_i^A<t<t_i^B, \\ 0, & t_i^B<t, \end{cases} \tag{4}$$

where t_i^A, t_i^B, and t_i^C denote the time of invasion of the ith site, the time at which the stock of nutrients at the site was exhausted, and the time at which the maximum age ϵ_{max} was reached, respectively. This behavior is illustrated in Fig. 3. For simplicity the constant A was set to a value of unity.

The age ϵ of a newly occupied site was set to 1.0. The age started to increased only after the nutrients at that site were exhausted ($t>t_i^B$ in Fig. 3). The ith cluster site aged according to a local time scale or ''biological clock,'' by the amount

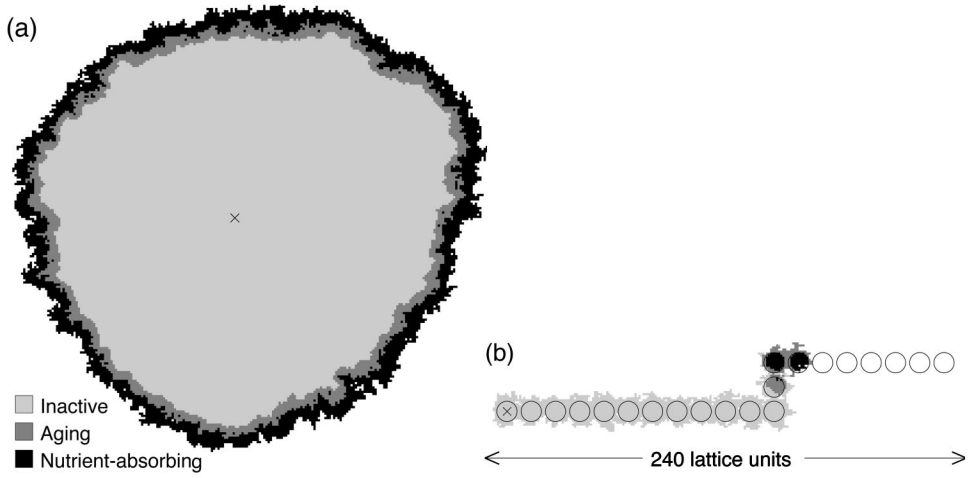

FIG. 4. (a) shows one stage during growth of a cluster on a uniform substrate of nutrients, and (b) a cluster growing along a line of nutrient-containing drops (circles) with a kink. Light, medium, and dark shades represent inactivated, active but nutrient-free, and active nutrient-containing cluster sites, respectively. The seed site is indicated by a cross. The model parameters were $n_0=3.0$, $\epsilon_{max}=6.0$, and $\alpha=3.0$. The drops in (b) had a diameter of 10 lattice units and were separated by 2 units.

$$\Delta\epsilon_i = d_i \Delta t, \tag{5}$$

where d_i is the distance from the ith site to the nearest nutrient-absorbing cluster site (occupied site at which the nutrients are not yet exhausted). Distances were defined as the number of lattice steps necessary to walk the shortest path consisting of steps between nearest-neighbor sites on the cluster. Equation (5) implies that well-nourished plasmodial regions age slowly, whereas regions far from nutrient sources age rapidly.

Recently occupied sites ($\epsilon<\epsilon_{max}$) were denoted ''active sites'' in the model. An occupied site became ''inactivated'' after reaching the maximum age ϵ_{max}. Inactivation of a site disabled local growth into unoccupied perimeter sites, since only unoccupied perimeter sites adjacent to an active cluster site could be invaded. The entire cluster became inactive if nutrient absorption was not possible at any of the cluster sites, and growth was stalled.

The coupling of local growth probabilities to the age of plasmodial regions, and thus to the spatial distribution of nutrients, leads to persistence in the growth process. Indeed, the cluster front is most likely to propagate in the vicinity of newly occupied sites with small ϵ [Eq. (1)]. The coupling of aging to nutrient supply [Eq. (5)] provides a feedback mechanism that favors propagation of the plasmodium into nutrient-rich regions of the substrate, and disfavors expansion into nutrient-free regions. This feedback leads to correlations in the spatial distribution of successive growth steps.

III. SIMULATIONS OF *PHYSARUM* GROWTH

Figures 4 and 5 show that this model reproduces the experimental observations (i)–(iv) listed in Sec. I. Figure 4(a) shows a cluster grown on a uniform substrate of nutrients. The cluster expands isotropically and consists of a core of inactivated sites ($\epsilon>\epsilon_{max}$). The core is surrounded by an inner halo of sites that are still active but have exhausted the local nutrient supply ($1.0<\epsilon<\epsilon_{max}$), and an outer halo of newly occupied sites at which nutrients can be absorbed ($\epsilon=1.0$). The resulting cluster is roughly circular and the mass of the halos increases approximately linearly in time. A real *Physarum* growing on a uniform agar substrate looks qualitatively similar [see Fig. 1(a)], but the halos are wider at the expense of the core of ''inactivated'' plasmodial regions. This is due to the slow diffusion of fresh nutrients from the interior of the nutrient-containing drops to their upper surfaces, where the nutrients become accessible to the *Physarum*. The diffusion of nutrients prolongs the duration of

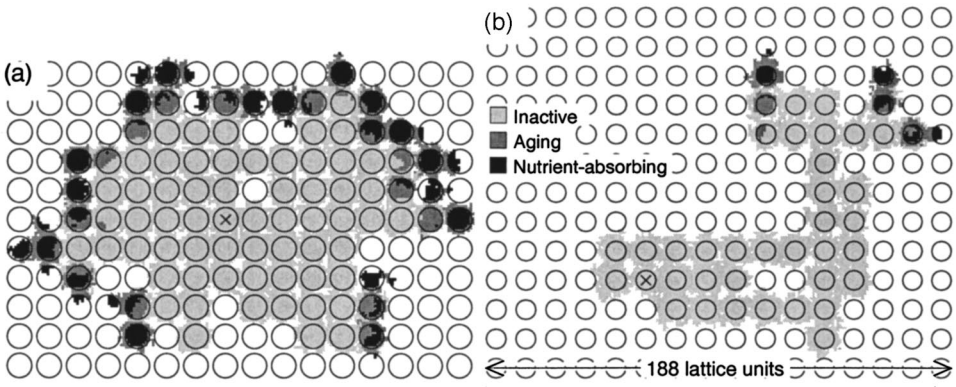

FIG. 5. Clusters grown on a square array of nutrient-containing drops (circles) with the parameters used to obtain Fig. 4. The center-to-center distance of the drops was 12 lattice units, and the drop diameters were 10 units in (a) and 8 units in (b). The seed site is indicated by a cross.

active behavior and can even lead to the reactivation of inactive regions. These effects were not taken into account in the simulations.

The parameters $n_0=3.0$, $\epsilon_{max}=6.0$, and $\alpha=3.0$ were used in the simulations discussed in this section. These values were chosen to achieve qualitative agreement with the experimental observations. However, on a uniform nutrient-containing substrate, all cluster sites in the outer halo are nutrient-containing sites and thus have the age of $\epsilon=1.0$. The value of α is irrelevant in this case since all growth steps are equally probable; see Eq. (1).

Figure 4(b) shows one stage in the growth of a cluster along an array of drops. To confirm the ability of the simulated plasmodium to locate new sources of nutrients, the drops formed a line with a kink. The cluster extended along the array of drops with a tail of inactivated sites. In the vicinity of the covered drops populated with active sites, ''searching structures'' were formed. These structures grew approximately isotropically around the most recently covered drop until fresh sites on a neighboring drop were encountered and occupied. Since these new cluster sites contained nutrients, they did not age initially ($\epsilon=1.0$), and sites adjacent to this branch of the searching structure were very likely to be occupied. Consequently, drops were covered rapidly after they were first contacted.

A quite different growth pattern is obtained if all cluster sites age at the same rate [replacing Eq. (5) by $\Delta\epsilon_i=\Delta t$], independent of the distance to the nearest occupied sites on which the nutrients have not been completely consumed. On a linear array of drops, the resulting cluster is wedge-shaped, since the searching structures protruding from the first drops grow without limits. This result is inconsistent with the experimental findings, where growth patterns very similar to the one shown in Fig. 4(b) were observed [33].

Figure 5 shows that various growth patterns can be observed on a regular array of nutrient-containing drops. The morphology of the growth patterns depended on the drop size. Large drops mediated compact but anisotropic cluster growth [Fig. 5(a)]. The clusters contained small holes or islands consisting of drops that were ''missed'' in the growth process. Connected regions of active, recently occupied sites extended over a considerable fraction of the entire cluster perimeter. With small drops [Fig. 5(b)], the active cluster sites were located at one or two centers that were isolated from each other and propagated on the substrate in the manner of random walkers. Several propagating branches were formed at some of the drops that had been covered by cluster sites. A branch whose propagation was stalled by random fluctuations (a branch that was missed in the random site selection process) was soon abandoned, since further growth became less and less probable. All but one branch could become inactivated, until a new bifurcation occurred. The cluster could not support a large number of active sites because of the long distances between nutrient-absorbing sites and remaining active zone sites. Most of the active sites aged rapidly. Under these conditions, the pattern formed by the covered drops was sparse.

The qualitative agreement between experiments and simulations is demonstrated by Figs. 6 and 7. These figures show plots of the number of covered drops as a function of the normalized growth time τ during a single experiment or simulation. Drop substrates with large drops and small drops, respectively, were used. The normalized growth time was given by $\tau=t/T_N$, where t is the time that had passed since the growth process started and T_N is the average time interval that elapsed in an experiment or a simulation between successive drop coverage events. The experimental data used

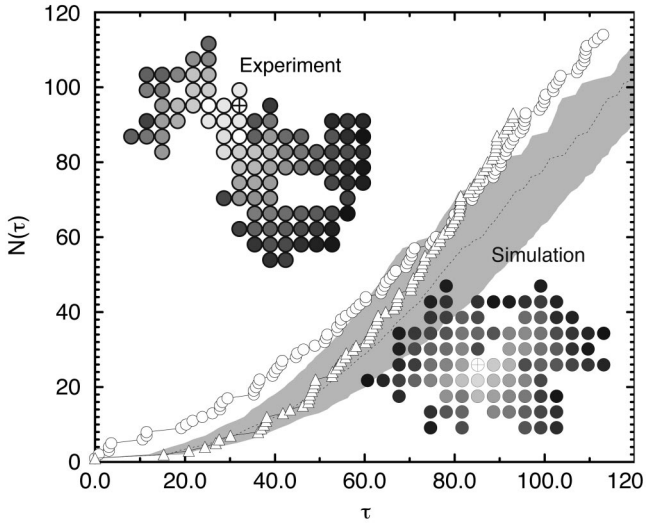

FIG. 6. Plots of the number of covered drops $N(\tau)$ as a function of the normalized time τ, observed in a single experiment (circles) and a single simulation (triangles) using drop substrates with large drops. The dotted line and shaded envelope indicate the mean and standard deviation observed in 20 simulations. The nutrient-containing drop coverage was 67% in the experiment and 55% in the simulation. The gray shades in the insets indicate the order of occupation, with dark shades representing the most recently occupied drops. The drop containing the seed site is marked by a cross.

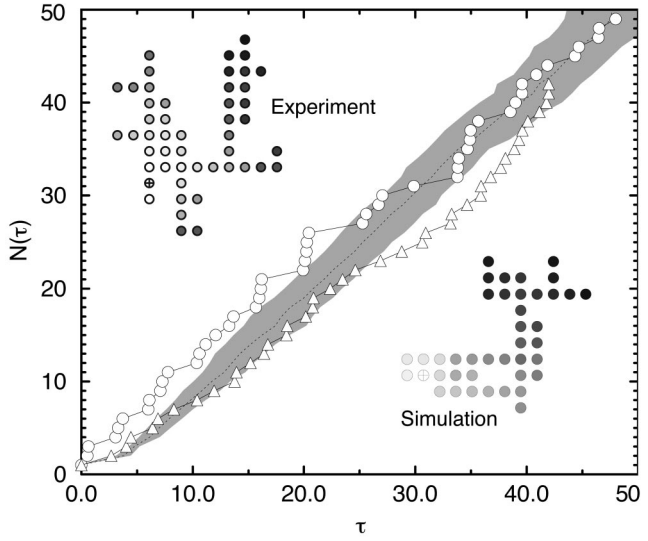

FIG. 7. Plots of the number of covered drops $N(\tau)$ as a function of the normalized time τ, observed in a single experiment (circles) and a single simulation (triangles) using drop substrates with small drops. The dotted line and shaded envelope indicate the mean and standard deviation observed in 20 simulations. The nutrient-containing drop coverage was 23% in the experiment and 35% in the simulation. The insets indicate the order of occupation, with dark shades representing the most recently occupied drops.

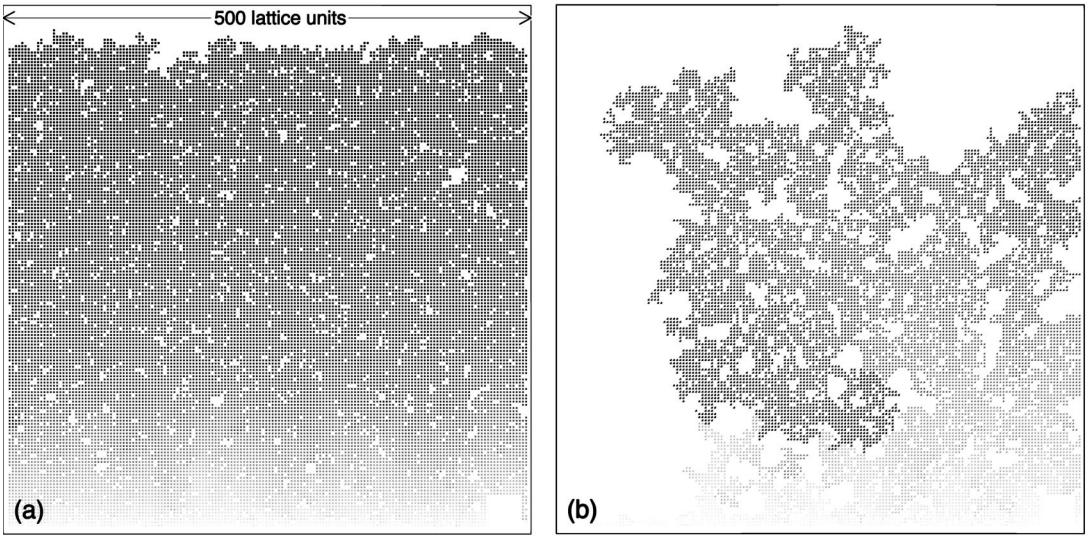

FIG. 8. Cluster growth sequences on drop substrates. Each nutrient-containing drop was represented by one lattice site and was separated by its nearest neighbor drops by two sites. To increase readability, only the covered drops are plotted, and they are enlarged by a factor of 2. The gray shades indicate the order of occupation, with darker shades representing the later invasions and bright shades representing drops that were occupied at early stages or not occupied at all. The cluster started to grow at a horizontal line of sites at the bottom boundary and propagated upward. Parts (a) and (b) show the patterns formed during growth using $\alpha=1.0$ and $\alpha=3.0$, respectively. The remaining model parameters were $n_0=2.0$ and $\epsilon_{max}=4.0$.

in Figs. 6 and 7 was taken from Ref. [33]. Except for the drop sizes, the simulation parameter used to obtain Figs. 6 and 7 were the same as those used in Figs. 4 and 5. Graphical illustrations of the sequence of drop invasion events are shown in the insets of Figs. 6 and 7. Experimental and simulated curves and invasion patterns share similar features, including anisotropic but compact growth at an increasingly faster coverage rate on large drops, and branched growth at an essentially constant drop coverage rate on small drops.

IV. SELECTED PROPERTIES

The simulation model is based on the idea that (i) growth occurs preferentially in young, recently formed regions of the plasmodium, and (ii) aging depends on the supply of nutrients. The growth strategy incorporated in the model is suitable for survival in an heterogeneous environment since propagation into nutritious regions persists and invasion of nutrient-poor regions is suppressed.

The degree of growth persistence is determined by the parameter α. For $\alpha=0$ and a sufficiently high maximum age ϵ_{max}, the cluster growth is like that of an Eden model cluster, while for $\alpha>0$, growth becomes increasingly persistent. On drop substrates, fresh drops are always found and invaded for Eden-like growth, and this leads to a continuous front of concentric searching structures. The searching structures become more sparse and thus more efficient in persistent growth, but fresh adjacent drops are more likely to be missed. In both cases, cluster growth can become terminated prematurely if n_0 or ϵ_{max} are low.

Figure 8 illustrates the sequence of drop invasion events obtained from simulations in which each drop was represented by only a single lattice site. Each drop was separated from its nearest-neighbor drops by a spacing of two lattice units, and the substrate contained 164×164 drops. The cluster could not grow across the boundaries of the substrate (nonperiodic boundary conditions). Cluster growth was initiated by simultaneously occupying one row of sites (including both nutrient-containing drop sites and nutrient-free substrate sites) at the bottom boundary of the substrate. Figures 8(a) and 8(b) correspond to weak persistence ($\alpha=1.0$) and intermediate persistence ($\alpha=3.0$), respectively. Weak persistence led to regular propagation of the cluster front, and only small patches of drops were left uncovered behind the front. All clusters eventually extended across the entire lattice in repeated simulations.

Intermediate or high persistence ($\alpha\geqslant3.0$) leads to irregular clusters containing numerous holes or islands of drops that remain uncovered during the growth process. Growth is concentrated onto a few well separated regions so that several propagating ''fingers'' are formed. Fingers can become trapped among inactivated cluster sites so that propagation comes to a halt, as may be seen in the lower central part of Fig. 8(b). Nevertheless, for $\alpha=3.0$, clusters always extended across the lattice.

For high persistence ($\alpha>3.0$), cluster growth was quickly reduced to the random propagation of a single finger. The probability $P(L,\alpha)$ that the cluster will extend across the lattice was found to decrease steeply with increasing L, so that one may speculate that $P(L\rightarrow\infty,\alpha>3)=0$. On the substrate of size $L=164\times164$ one-site drops, the spanning probability is quite small ($P=0.27$ and $P=0.03$ for $\alpha=4.0$ and $\alpha=5.0$, respectively).

Figure 9 shows a plot of the number of active sites N_a counted during cluster growth across a drop substrate with one-site drops. The simulations started like those shown in Fig. 8, by occupying a line of sites along the bottom edge of the substrate. The nutrient supply of a fresh drop was $n_0=2.0$ and the lifetime of a cluster site was $\epsilon_{max}=4.0$. N_a reached a maximum shortly after start of the simulation (see

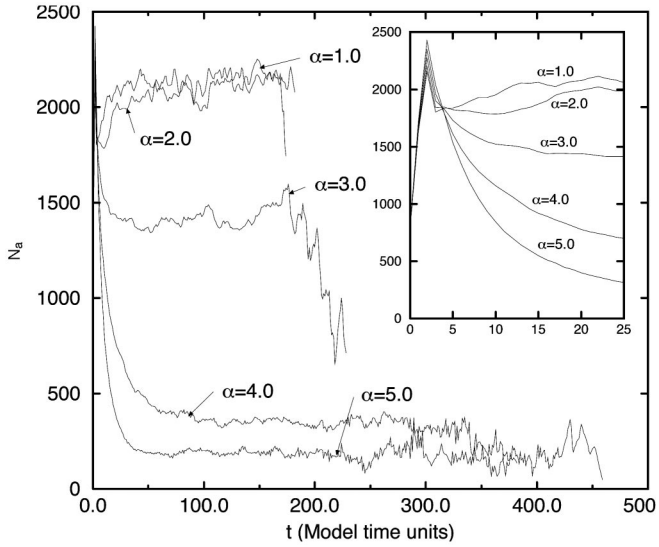

FIG. 9. Plots of the number of active sites N_a as a function of time t during cluster growth, averaged over several dozens of runs. The persistence parameter α was varied. The drop geometry and other model parameters were the same as those used to obtain Fig. 8. The initial configuration consisted of 164 occupied one-site drops and 328 occupied nutrient-free sites that formed a straight line at the boundary of the 164×164 one-site drop substrate. The inset shows $N_a(t)$ during the initial stages.

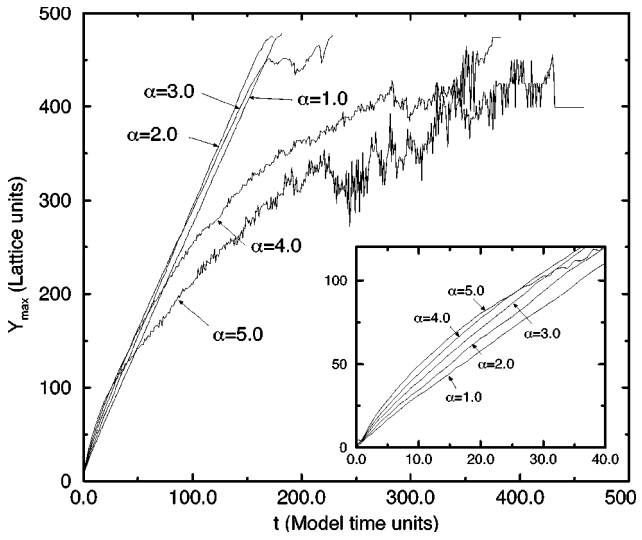

FIG. 10. Plot of the coordinate Y_{max} of the most advanced region occupied in the growth process as a function of time t during cluster growth from a line of occupied sites at $Y=0$ with blocking boundaries in the X-direction. The results from several dozen runs were averaged, and the persistence parameter α was varied. The drop geometry and other model parameters were the same as those used to obtain Fig. 8. The inset shows $Y_{max}(t)$ during the initial stages.

the inset of Fig. 9). At later times the average, taken over individual runs, appeared to approach a time-independent value.

Initially, propagation occurred along the entire front with equal probability, since all seed sites were of the same age. This led to an Eden-like growth process, and both N_a and s initially increased as the cluster front roughened. Propagation of the front occurred preferentially in regions where growth had recently occurred. The occupation probabilities of the unoccupied perimeter sites were nonuniformly distributed along the advancing front, after the initial transient behavior had decayed.

For $\alpha\geqslant3.0$, the occupation probabilities were so unevenly distributed that only a fraction of the sites on the unoccupied perimeter participated in the growth process while entire sections of the front became inactivated. Both the number of active sites N_a and the number of possible growth steps s dropped rapidly. The cluster's clock then operated at a faster speed [Eq. (3)] so that aging of fresh sites was accelerated. The collapse of N_a was counteracted by the fact that growth was likely to occur in the vicinity of most of the few surviving active sites, since the number of remaining possible steps was small. The new occupations supported further growth steps so that the front length increased and the cluster's clock speed slowed down. These mechanisms led to large fluctuations in both the number of active sites N_a and the number of possible growth steps s. Growth was often terminated prematurely because the fluctuations of N_a became large enough, relative to the mean value, for the number of active sites to reach zero. As α was increased, the arrival time increased significantly for the fraction of clusters that reached across the entire substrate.

For $\alpha\leqslant2.0$, N_a and s fluctuated much less and a belt of active sites formed that extended across the entire substrate. The mass of the belt was approximately constant in each run after a transient period.

In an environment where nutrients are scarce, such as the regular drop substrate used in the experiments [33], propagation velocity is an important factor. Fast propagation shortens the period of starvation, until fresh regions with abundance of nutrients are located. Figure 10 shows a plot of the coordinate Y_{max} of the invaded drop that is most distant from the starting line, at each stage t. The slope $dY_{max}(t)/dt$ is a measure of the net propagation velocity of the clusters. [It is, however, not a measure of the *local* front propagation velocity with which fingers of a discontinuous front may grow along tortuous paths. That local velocity is much larger than $dY_{max}(t)/dt$, because the growth probability distribution is concentrated onto a few points.]

At low and intermediate degrees of persistence ($\alpha\leqslant3.0$), the net propagation velocity was approximately constant, until the cluster reached the lattice boundary. At higher α, the average propagation velocity decreased rapidly with time, due to trapping of propagating fingers and the tortuous paths taken by the active fragments of the growth front at the tips of the propagating fingers. However, during the initial stages, a high degree of persistence led to fast propagation. This is shown in more detail in the inset of Fig. 10. The state of intermediate persistence appeared to combine fairly rapid propagation with a high probability to extend across the low-nutrient content environment.

V. DISCUSSION

The starting point of this work was an experimental study of the growth behavior of *Physarum* in environments with a nonuniform distribution of nutrients. Growth in such an environment cannot be represented by a simple Eden model,

because the Eden model cannot be used to simulate adjustment to varying conditions, such as the concentration of nutrients. Moreover, the concepts of ''aging'' and ''inactivation'' are not inherent in the Eden model.

In this work we studied a modified Eden model with an *ad hoc* time scale. The rate of aging of cluster sites was influenced by the distance to the nearest source of nutrients. The probability that a given unoccupied perimeter site will be occupied depended on the age of the adjacent cluster sites. By construction, this approach leads to a cluster growth that favors growth in the most nutritious parts of the substrate, and that grows persistently in the sense that growth is more likely to occur close to recently occupied regions. Persistence in the selection of growth directions, due to the coupling between the influences of age and of local nutrients supply on the selection of growth sites, is a crucial element of the growth model. The model successfully reproduces salient features associated with the growth of *Physarum*, including the isotropic expansion of a sedentary plasmodium on a uniform, nutritious substrate, and the selective coverage of nutrient-containing drops on a non-uniform substrate.

Persistence alone cannot secure survival in an inhomogeneous environment, such as the drop substrates considered here. It must be balanced by a tendency to explore fresh regions systematically and in all directions, in order to maximize the amount of nutrients that can be taken up at each stage. In our model, the balance is described by the parameter α. Indeed, we found that the value of $\alpha = 3.0$, leading to an intermediate degree of persistence, is significant in two respects. First, a value of about 3.0 for α led to the best agreement with the experimental growth patterns on a range of substrate types. Lower values of α failed to reproduce branched patterns such as the one shown in Fig. 1(d) and in the inset of Fig. 7, whereas growth along a line of drops [Fig. 4(b)] could not be achieved using high values of α. Second, $\alpha = 3.0$ led to a high propagation velocity during the early stages of growth on large lattices, while maintaining a high probability to reach across the entire lattice at later stages. From this point of view, an intermediate degree of persistence may be best suited in such an environment.

The model considered in this paper exhibits growth correlations over a length scale ξ. The mean separation of sites that are occupied in successive growth steps is a measure of ξ. For low values of α, the degree of persistence is low, and sites occupied in subsequent steps are not necessarily close to each other. Indeed, in the case of $\alpha = 0$, the age ϵ of cluster sites is irrelevant and the correlation length ξ is of the order of the diameter of the cluster of occupied sites. The same applies to the case of growth on a uniform, nutritious substrate, as shown in Fig. 4(a), in which all cluster sites adjacent to the cluster front are of age $\epsilon = 1.0$. In contrast, at high α, growth on nonuniform substrates is highly persistent, so that ξ is of the order of only a few lattice units. In that case, the cluster front fragments into several active segments that propagate independently, as shown in Fig. 8(b).

Naturally emerging correlation lengths that adjust to different environments must be part of any model of the growth and functioning of *Physarum*. It is, for instance, well known that the ectoplasmic contractions in *Physarum* are synchronized under stable conditions, not only in excised fragments [37] but also within intact, sedentary plasmodia which measure several centimeters across [38,39]. On a drop substrate, however, the contractions in plasmodial regions residing on adjacent drops are poorly synchronized, and the phase between the rhythms displays large deviations, occasionally exceeding 90° [32]. The variability of synchronization indicates that it is useful to think about cellular activities (such as ectoplasmic contractions) in terms of a correlation length ξ' (not necessarily related to the growth correlation length ξ in the model). One strategy to study the growth and functioning of giant cells such as *Physarum* may thus be to identify spatially or temporally correlated events, and then to ask what mechanisms control the correlations. It is possible that drop substrates are suitable tools to this end.

In summary, a stochastic model of plasmodial growth, based on the Eden growth model, and supported by experimental studies, is presented. This model is very simple relative to the complexity of processes that control the propagation of *Physarum*. An extension of the model might focus of the continuous diffusion of nutrients from the interior to the surface of the drops, possibly leading to ''reactivation'' of inactivated sections of the plasmodium. In fact, it appeared in some of the experiments that seemingly inactive parts of a plasmodium could become revitalized. For instance, in growth on a circular array of drops, the growth direction changed spontaneously in some cases. In contrast, in simulations such as the one shown in Fig. 8, trapping of propagating ''fingers'' occurred with increasing frequency as α was increased and fingers became more pronounced. For $\alpha \geqslant 4.0$, one or only few fingers propagated simultaneously, and the entire cluster could become inactivated upon trapping. A second extension of the model may involve mechanisms that relate growth directions to stimuli such as concentration gradients of water or poison, a response known to occur in experiments [40].

ACKNOWLEDGMENTS

We thank Kim Christensen for helpful comments. We gratefully acknowledge support by VISTA, a research cooperation between the Norwegian Academy of Science and Letters, and Den norske stats oljeselskap a.s. (STATOIL), and by the Research Council of Norway (NFR). The work presented here has received support from the NFR through a grant of computing time.

[1] M. Eden, in *Proceedings of the 4th Berkeley Symposium on Mathematical Statistics and Probability*, edited by J. Neyman (University of California Press, Berkeley, 1961), pp. 223–239.

[2] A. L. Barabasi and H. E. Stanley, *Fractal Concepts in Surface Growth* (Cambridge University Press, Cambridge, 1995).

[3] P. Meakin, *Fractals, Scaling, and Growth Far From Equilibrium* (Cambridge University Press, Cambridge, 1998).

[4] T. Williams and R. Bjerknes, Nature (London) **236**, 19 (1972).

[5] E. Ben-Jacob, O. Shochet, I. Cohen, A. Tenenbaum, A. Czirok, and T. Viscsek, Fractals **3**, 849 (1995).

[6] W. Ziqin and L. Boquan, Phys. Rev. E **51**, R16 (1995).
[7] A. Czirok, E. Ben-Jacob, I. Cohen, and T. Vicsek, Phys. Rev. E **54**, 1791 (1996).
[8] K. Kawasaki, A. Mochizuki, M. Matsushita, T. Umeda, and N. Shigesada, J. Theor. Biol. **188**, 177 (1997).
[9] M. Matsuhita, J. Wakita, H. Hoh, I. Rafols, T. Matsuyama, H. Sakaguchi, and M. Mimura, Physica A **249**, 517 (1998).
[10] J. Halley, H. Comins, J. Lawton, and M. Hassell, OIKSAA **70**, 435 (1994).
[11] F. A. Davidson, B. D. Sleeman, A. D. M. Rayner, J. W. Crawford, and K. Ritz, Proc. R. Soc. London, Ser. B **263**, 873 (1996).
[12] H. Meinhardt, *Models of Biological Pattern Formation* (Academic Press, London, 1982).
[13] A. J. Koch and H. Meinhardt, Rev. Mod. Phys. **66**, 1481 (1994).
[14] D. Young and E. Corey, Phys. Rev. A **41**, 7024 (1990).
[15] J. Garcia-Ruiz, E. Louis, M. P., and L. E. Sander, *Growth Patterns in Physical Sciences and Biology*, NATO ASI Series, B304 (Plenum Press, New York, 1993).
[16] A. Deutsch, Int. J. Bifurcation Chaos Appl. Sci. Eng. **6**, 1735 (1996).
[17] T. Sams, K. Sneppen, M. H. Jensen, C. Ellegaard, B. E. Christensen, and U. Thrane, Phys. Rev. Lett. **79**, 313 (1997).
[18] A. Czirok, H. E. Stanley, and T. Vicsek, J. Phys. A **30**, 1375 (1997).
[19] S. Tohya, A. Mochizuki, S. Imayama, and Y. Iwasa, J. Theor. Biol. **194**, 65 (1998).
[20] I. Derény and T. Vicsek, Physica A **249**, 397 (1998).
[21] A. Czirok, K. Schlett, E. Madarasz, and T. Vicsek, Phys. Rev. Lett. **81**, 3038 (1998).
[22] D. A. Kessler and H. Levine, Phys. Rev. E **48**, 4801 (1993).
[23] T. Höefer, J. A. Sherratt, and P. K. Maini, Physica D **85**, 425 (1995).
[24] H. Levine, Physica A **249**, 53 (1998).
[25] J. Bailey, Microbiology (UK) **141**, 2355 (1995).
[26] H. W. Sauer, *Developmental Biology of Physarum* (Cambridge University Press, Cambridge, England, 1982).
[27] J. M. Ashworth and J. Dee, *The Biology of Slime Moulds* (Edward Arnold, Ltd., London, 1975).
[28] E. Guttes and S. Guttes, in *Methods in Cell Physiology*, edited by D. M. Prescott (Academic Press, New York, 1964), pp. 43–54.
[29] W. Stockem and K. Brix, Int. Rev. Cytol. **149**, 145 (1994).
[30] N. Kamiya, Annu. Rep. Biol. Works Fac. Sci. Osaka Univ. **1**, 53 (1953).
[31] J. Dee, Sci. Prog. **62**, 523 (1975).
[32] R. Halvorsrud, I. Giaever, and J. Feder, Biological Rhythm Res. **28**, 358 (1997).
[33] R. Halvorsrud and G. Wagner, Phys. Rev. E **57**, 941 (1998).
[34] J. J. Tyson, in *Cell Biology of Physarum and Didymium*, edited by H. C. Aldrich and J. W. Daniel (Academic Press, New York, 1982), Vol. I, pp. 61–110.
[35] R. Jullien and R. Botet, Phys. Rev. Lett. **54**, 2055 (1985).
[36] U. Oxaal (private communication).
[37] Y. Takeuchi and M. Yoneda, J. Cell. Sci. **26**, 151 (1977).
[38] A. Grebecki and M. Cieślawska, Cytobiologie **17**, 335 (1978).
[39] R. Halvorsrud, M. M. Laane, and I. Giaever, Biological Rhythm Res. **26**, 316 (1995).
[40] T. Ueda and Y. Kobatake, in *Cell Biology of Physarum and Didymium*, edited by H. C. Aldrich and J. W. Daniel (Academic Press, New York, 1982), Vol. I, pp. 111–143.